Metal Complexes of Severely Crowded Molecules. Synthesis, Structure, and Reactivities of the $M(CO)_3$ (M = Cr, Mo, and W) Complexes of Octamethylnaphthalene

John W. Hull, Jr., and Wayne L. Gladfelter*

Department of Chemistry, University of Minnesota, Minneapolis, Minnesota 55455

Received July 7, 1981

The preparations of the metal tricarbonyl complexes (Cr, Mo, and W) of octamethylnaphthalene (OMN) are described. The structure of the chromium complex was determined by single-crystal X-ray crystallography [$P\bar{1}$ space group, $Z = 2$, $a = 9.326$ (4) Å, $b = 13.992$ (3) Å, $c = 7.919$ (2) Å, $\alpha = 95.44$ (2)°, $\beta = 115.00$ (3)°, $\gamma = 76.40$ (2)°]. The chromium tricarbonyl fragment is π bound to one the six-membered rings. The distortions of the metal-complexed OMN differ very little from the structure of the free ligand. The thermal and photochemical reactions of the Cr complex with phosphorus donor ligands differed. Photolysis of $(OMN)Cr(CO)_3$ in the presence of triphenylphosphine produces purple $(OMN)Cr(CO)_2PPh_3$, while heating $(OMN)Cr(CO)_3$ in neat trimethyl phosphite generates $Cr(CO)_3[P(OCH_3)_3]_3$. Maleic anhydride reacts with $(OMN)Cr(CO)_3$ to give two isomers resulting from a Diels–Alder addition to the free ring. The stereochemistry of one of the isomers was determined by X-ray crystallography [$P2_1/c$ space group, $Z = 4$, $a = 16.219$ (6) Å, $b = 9.284$ (3) Å, $c = 16.718$ (6) Å, $\beta = 118.07$ (3)°] and was found to result from attack of maleic anhydride on the side of the ring opposite the metal atom. The two isomers differ in the orientation (exo and endo) of the anhydride group with respect to the aromatic ring. A comparison of the equilibrium constants for the free ligand and the complex in the Diels–Alder reaction shows an enhancement of over 2 orders of magnitude for the metal complex. The difference is attributed to the increased strength of interaction of the metal with the planar ring of the cycloaddition product.

Introduction

When substituents are placed in the peri positions of naphthalene, a molecular distortion ensues caused by nonbonding repulsive forces between these groups. By changing the substituents, it has been possible to change both the magnitude and even the mode of the distortions.[1] At the extremes, two types are found. The first involves an in-plane bend of the C1– and/or the C8–substituent bond, I. The second involves a displacement of the sub-

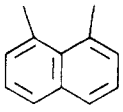

I

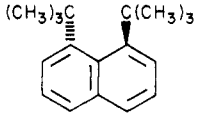

II

stituents above and below the mean plane of the naphthalene ring, II. 1,8-Dimethylnaphthalene exhibits an in-plane distortion[2] while larger groups such as bis(trimethylelement) (C, Ge, and Sn) force the out-of-plane distortion to occur.[3–7] The structural details of many of these compounds have been examined by X-ray crystallography[2,3,5,8–10] and evaluated by using force field calculations.[3,5,7] Molecules of the second type have the additional interesting feature of chirality. The barriers for enantiomerization are typically too low to allow observation for all but the bulkiest groups such as $[(CH_3)_3Z]_2$, where Z = C, Ge, and Sn. Although the value of $\Delta G^{\ddagger}$ for Z = C is estimated to be greater than 24 kcal/mol,[4] the measured value for 1,8-bis(trimethylgermyl)-4-(methoxymethyl)-naphthalene is 7.5 ± 0.1 kcal/mol at −122 °C.[7]

Octamethylnaphthalene (OMN) fits into a subclass of these systems in which both sets of peri positions are substituted. After its synthesis[11] in 1953, a single-crystal X-ray crystallographic study showed[12] that unlike 1,8-dimethylnaphthalene, OMN distorts in an out-of-plane fashion. This study also suggested that the structure is that shown in III, but this was later questioned after a

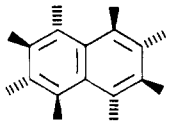

III

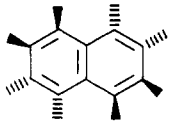

IV

study of octachloronaphthalene revealed[13] that the chloro substituents are distorted in a pairwise fashion, IV. Hart and co-workers recently published[14] an efficient synthesis of OMN and upon reinvestigating the X-ray crystallographic analysis indeed found that the molecule has the structure shown in IV.[15]

The effect of metal complexation of arenes on the conformation of the ligand itself recently was examined by Mislow and co-workers[16] in the chromium tricarbonyl complex of hexaethylbenzene. In solution and the solid-state structure of $(\eta^6\text{-}C_6Et_6)Cr(CO)_3$ the methyls are pos-

(1) Balasubramaniyan, V. *Chem. Rev.* **1966**, *66*, 567.
(2) Bright, D.; Maxwell, I. E.; deBoer, J. *J. Chem. Soc., Perkin Trans. 2* **1973**, 2101.
(3) Handal, J.; White, J. G.; Franck, R. W.; Yuh, Y. H.; Allinger, N. L. *J. Am. Chem. Soc.* **1977**, *99*, 3345.
(4) Anderson, J. E.; Franck, R. W.; Mandella, W. L. *J. Am. Chem. Soc.* **1972**, *94*, 4608.
(5) Blount, J. F.; Cozzi, F.; Damewood, J. R., Jr.; Iroff, L. D.; Sjöstrand, U.; Mislow, K. *J. Am. Chem. Soc.* **1980**, *102*, 99.
(6) Anet, F. A. L.; Donovan, D.; Sjöstrand, U.; Cozzi, F.; Mislow, K. *J. Am. Chem. Soc.* **1980**, *102*, 1748.
(7) Hounshell, W. D.; Anet, F. A. L.; Cozzi, F.; Damewood, J. R., Jr.; Johnson, C. A.; Sjöstrand, U.; Mislow, K. *J. Am. Chem. Soc.* **1980**, *102*, 5941.
(8) Einspuhr, H.; Robert, J. B.; Marsh, R. E.; Roberts, J. D. *Acta Crystallogr., Sect. B* **1973**, *B29*, 1611.
(9) Robert, J. B.; Sherfinski, J. S.; Marsh, R. E.; Roberts, J. D. *J. Org. Chem.* **1974**, *39*, 1152.
(10) Herbstein, F. H. *Acta Crystallogr., Sect. B* **1979**, *B35*, 1661.
(11) Abadir, J. B.; Cook, J. W.; Gibson, D. T. *J. Chem. Soc.* **1953**, 8.
(12) Donaldson, D. M.; Robertson, J. M. *J. Chem. Soc.* **1953**, 17.
(13) Gafner, G.; Herbstein, F. H. *Nature (London)* **1963**, *200*, 130.
(14) Hart, H.; Teuerstein, A. *Synthesis* **1979**, 693.
(15) Hart, H., personal communication.
(16) Hunter, G.; Iverson, D. J.; Mislow, K.; Blount, J. F. *J. Am. Chem. Soc.* **1980**, *102*, 5942.

0276-7333/82/2301-0264$01.25/0 © 1982 American Chemical Society

itioned alternatively above and below the plane of the arene. Upon substitution of only one carbonyl with triphenylphosphine all the methyls were forced to the side of the ring which was opposite that of the metal.

We have initiated a study of the interaction of transition metals with severely crowded naphthalenes and report here our results on the synthesis, structure, and reactivity of (octamethylnaphthalene)tricarbonylmetal (M = Cr, Mo, and W) complexes.

Experimental Section

General Information. ^{1}H NMR spectra were obtained on Varian Models CFT-20 and XL-100, as well as a Bruker 270 MHz instrument. Infrared spectra were obtained on a Beckman Model 4250. All solvents were freshly distilled over sodium benzophenone ketyl under nitrogen atmosphere unless stated otherwise. All metal hexacarbonyls were purchased from Strem Chemical Co. Octamethylnaphthalene[14] and $(CH_3CN)_3M(CO)_3$ (M = Mo, W)[17,18] were prepared by using literature procedures. All elemental analysess were obtained from Galbraith Laboratories.

(Octamethylnaphthalene)tricarbonylchromium(0). Hexacarbonylchromium (2.1 g, 9.6 mmol) and OMN (2.3 g, 9.6 mmol) were placed into a 250-mL round-bottom flask, and dry di-*n*-butyl ether (125 mL) was distilled into the reaction flask, followed by 7 mL of dry tetrahydrofuran (THF). After being fitted with a reflux condenser, the system was stirred, flushed with N_2, and refluxed. After 24 h the solution was cooled, filtered through a 2-cm layer of silica gel placed on a glass frit, and then rinsed with a few milliliters of benzene. The solvent was removed on a rotary evaporator with a 90 °C water bath to yield a dark red solid. Recrystallization in benzene/hexane yielded dark red crystals (52%) which are stable to air. Anal. Calcd for $C_{21}H_{24}CrO_3$: C, 67.00; H, 6.44. Found: C, 67.07; H, 6.61.

(Octamethylnaphthalene)tricarbonylmolybdenum(0). Tris(acetonitrile)tricarbonylmolybdenum (0.44 g, 1.5 mmol) was weighed into a Schlenk tube in an inert-atmosphere glovebox. Octamethylnaphthalene (0.42 g, 1.8 mmol) and dried, deoxygenated hexane (20 mL) were added. A condenser was attached to the Schlenk tube, and refluxing was maintained for 12 h, with constant magnetic stirring. The solution was filtered hot under N_2, leaving insoluble $(OMN)Mo(CO)_3$ as an orange, slightly air-sensitive solid on the filter (ca. 30% yield). Recrystallization in dry, deoxygenated CH_2Cl_2/hexane yielded bright orange crystals. Anal. Calcd for $C_{21}H_{24}MoO_3$: C, 60.00; H, 5.76. Found: C, 60.15; H, 5.85.

(Octamethylnaphthalene)tricarbonyltungsten(0). Tris(acetonitrile)tricarbonyltungsten (1.14 g, 2.91 mmol) and OMN (0.91 g, 3.78 mmol) were refluxed in 40 mL of dry hexane under nitrogen atmosphere for 8 days. After heating was stopped, the solution was filtered through a glass frit, followed by a hexane rinse. The filter flask was then changed, and the solid mass on the frit was rinsed repeatedly with methylene chloride to wash out bright red $(OMN)W(CO)_3$. The solid obtained after evaporation was recrystallized in dry, degassed CH_2Cl_2/hexane to give bright orange-red crystals (0.26 g, 18% yield). Anal. Calcd for $C_{21}H_{24}O_3W$: C, 49.63; H, 4.76. Found: C, 49.45; H, 4.79.

(Octamethylnaphthalene)dicarbonyl(triphenylphosphine)chromium(0). (Octamethylnaphthalene)tricarbonylchromium (0.27 g, 0.72 mmol) and triphenylphosphine (0.56 g, 2.15 mmol, recrystallized from ethanol) were irradiated in 30 mL of dry hexane in a Schlenk tube with a Hanovia ultraviolet lamp for 8 h. The heat from the lamp was allowed to reflux the reaction mixture, and good stirring was maintained under a N_2 atmosphere. The dark violet solution was filtered hot through a glass frit and rinsed with hexane to obtain 0.15 g (34%) of a violet solid which is stable to air. Recrystallization in dry, degassed CH_2Cl_2/hexane yielded large, dark violet crystals. Anal. Calcd for $C_{38}H_{39}CrPO_2$: C, 74.74; H, 6.44. Found: C, 75.00; H, 6.56.

Tricarbonyltris(trimethyl phosphite)chromium. (Octamethylnaphthalene)tricarbonylchromium (30.5 mg, 0.08 mmol) was warmed to 70 °C in 2 mL of trimethyl phosphite under a nitrogen atmosphere. After being stirred for 2 h, the solution was cooled in an ice bath. Octamethylnaphthalene crystallized from the solution and was filtered off, after which trimethyl phosphite was removed by vacuum distillation. The resulting light-colored solid was rinsed with cold hexane, dried under vacuum, and obtained in 57% yield as a moderately air-sensitive solid. Infrared analysis indicated the presence of predominantly the facial isomer.[19]

[1,4,5,6-Tetramethyl-7,8-(tetramethylbenzo)bicyclo[2.2.2]octa-5,7-diene-2,3-dicarboxylic anhydride]tricarbonylchromium ([OMN·MA]Cr(CO)$_3$). (Octamethylnaphthalene)tricarbonylchromium (601 mg, 1.6 mmol) and maleic anhydride (783 mg, 8.0 mmol) were placed into a 25-mL round-bottom flask; a reflux condensor fitted with a gas stopcock was attached and the system was repeatedly evacuated and flushed with nitrogen on a Schlenk line. Dry benzene (15 mL, distilled over CaH_2) was added quickly by syringe through the top of the condensor. The dark red solution was allowed to reflux under a nitrogen atmosphere with magnetic stirring for 21 h, by which time the color had lightened considerably to orange-red. The solution was cooled to room temperature and the benzene evaporated leaving a red-yellow solid, which was completely redissolved in about 10 mL of dry THF. Hexane was then added to the cloud point, and the flask was cooled in a freezer. The first crop of yellow crystals (206 mg) consisted of mainly the exo isomer. A second crop (174 mg) obtained from the mother liquor consisted of mainly the endo isomer. After the second crop was isolated, the yellow filtrate was washed with two or three small portions of water to remove excess maleic anhydride, dried over $MgSO_4$, and reduced in volume. An additional 198 mg of yellow crystals consisting of mostly endo isomer was obtained, giving a total isolated yield of 578 mg (76%). Complete separation of isomers was readily accomplished on a silica gel column, eluted with 3/1 hexane/ethyl acetate. The exo isomer eluted fairly rapidly, followed by the much slower endo isomer. Recrystallization in THF/hexane afforded completely pure $(OMN{\cdot}MA)Cr(CO)_3$ as the single isomers by the HPLC analysis. The final exo/endo ratio is 2.3. Anal. Calcd for $C_{25}H_{26}CrO_6$: C, 63.29; H, 5.52. Found: C, 64.11; H, 5.73.

1,4,5,6-Tetramethyl-7,8-(tetramethylbenzo)bicyclo[2.2.2]octa-5,7-diene-2,3-dicarboxylic Anhydride (OMN·MA). A. From Octamethylnaphthalene. Octamethylnaphthalene (584.6 mg, 2.43 mmol) and reagent grade maleic anhydride (7.15 g, 73.0 mmol) were placed into a 50-mL round-bottom flask, and 25 mL of benzene was added. The solution turned immediately to a bright red color due to formation of the charge-transfer complex. The solution was refluxed with magnetic stirring for 65 h, after which the solvent was evaporated to give a yellow solid. Water was added to the flask with stirring to dissolve excess maleic anhydride. Diethyl ether was added, and the contents were transferred to a separatory funnel. The organic layer was extracted twice with water and then evaporated to a white solid. Recrystallization in methylene chloride/hexane afforded 486 mg (59%) of both exo and endo isomers in a ratio of 7:1.

B. From (Octamethylnaphthalene–maleic anhydride)tricarbonylchromium. The readily separated $(OMN{\cdot}MA)Cr(CO)_3$ isomers can be treated to obtain the corresponding OMN·MA adducts as single isomers.[20] Thus, a single isomer of $(OMN{\cdot}MA)Cr(CO)_3$ was irradiated in THF in the presence of oxygen with a Hanovia ultraviolet quartz lamp in a round-bottom flask with magnetic stirring. The flask was cooled with a rapid stream of air to prevent any retro-Diels–Alder reaction from occurring. After 6–8 h of irradiation, the resulting cloudy green solution was filtered through a glass frit containing a layer of diatomaceous earth, and the clear, colorless solution was evaporated to a white solid. Recrystallization in THF/hexane afforded a single isomer of pure (OMN·MA) adduct in essentially quantitative yield from $(OMN{\cdot}MA)Cr(CO)_3$.

HPLC Analysis of Diels–Alder and Retro-Diels–Alder Reactions. High-pressure liquid chromatography was performed with a Waters Associates M-45 solvent delivery system equipped with a Rheodyne 7125 injector and Beckman 153 UV analytical detector. A Waters Associates 30-cm μPorasil silica column af-

(17) King, R. B. *J. Organomet. Chem.* **1967**, *8*, 139.
(18) Tate, D. L.; Knipple, W. R.; Aigl, J. M. *Inorg. Chem.* **1962**, *1*, 433.
(19) Mathieu, R.; Lenzi, M.; Poilblanc, R. *Inorg. Chem.* **1970**, *9*, 2030.
(20) Jaouen, G. *Ann. New York Acad. Sci.* **1977**, *295*, 59.

Table I. Data for the X-ray Diffraction Study of (OMN)Cr(CO)$_3$

Crystal Parameters

crystal system = triclinic	V = 910 (1) Å^3
space group = $P\bar{1}$	Z = 2
a = 9.326 (4) Å	calcd density = 1.37 g cm^{-3}
b = 13.992 (3) Å	temp = 22 °C
c = 7.919 (2) Å	abs coeff = 6.73 cm^{-1}
α = 95.44 (2)°	formula = $C_{21}H_{24}CrO_3$
β = 115.00 (3)°	
γ = 76.40 (2)°	

Measurement of Intensity Data

diffractometer = Enraf-Nonius CAD4
radiation = Mo Kα (λ = 0.710 69 Å)
monochrometer = graphite crystal
scan speed = variable, see text
scan range = 0° $\leqslant 2\theta \leqslant$ 50°
reflections measd = $\pm h, \pm k, +l$
check reflections = {0,8,0}, {6,0,0}, {3,3,−3}; measured every 1.5 h
reflections collected = 3221 unique reflections; 2665 with $I > 2.5\sigma(I)$
p = 0.05
R = 2.9%
R_w = 4.4%

Table II

Crystal Parameters

crystal system = monoclinic	V = 2221 (3) Å^3
space group = $P2_1/c$	Z = 4
a = 16.219 (6) Å	calcd density = 1.42 g cm^{-3}
b = 9.284 (3) Å	formula = $C_{25}H_{26}CrO_6$
c = 16.718 (6) Å	temp = 22 °C
β = 118.07 (3)°	abs coeff = 5.80 cm^{-1}

Measurement of Intensity Data

diffractometer = Enraf-Nonius CAD4
radiation = Mo Kα (λ = 0.710 69 Å)
monochrometer = graphite crystal
scan speed = variable, see text
scan range = 0° $\leqslant 2\theta \leqslant$ 50°
reflections measd = $+h, +k, \pm l$
check reflections = {8,0,0}, {−2,−4,−1}, {0,2,6}; measured approximately every 150 reflections
reflections collected = 4319 unique reflections; 2013 with $I > 2.5\sigma(I)$
p = 0.03
R = 0.048
R_w = 0.048

forded baseline separation of reaction components, eluting with a 4/1 hexane/ethyl acetate solvent mixture (MCB glass distilled, filtered through 5 μm glass frit prior to use) at a rate of 3.0 mL/min (1500 psi). Stock solutions of OMN, OMN·MA (each isomer), (OMN)Cr(CO)$_3$, and (OMN·MA)Cr(CO)$_3$ (each isomer) in THF were injected at various concentrations to determine standard concentration curves from peak heights and peak areas.

A. Chromium Complexes. One-milliliter solutions of the complexes in benzene were prepared as in the (OMN·MA)Cr(CO)$_3$ synthesis. Contact of dissolved substrates with oxygen and moisture was scrupulously avoided. A typical run was as follows. (OMN)Cr(CO)$_3$ (10.8 mg, 0.029 mmol) and maleic anhydride (14.1 mg, 0.143 mmol) were refluxed in 1.0 mL of benzene under N_2 with magnetic stirring for 26 h. Benzene was evaporated on a rotary evaporator, and the solid was redissolved in 1.0 mL of dry THF for HPLC analysis. (The adducts are more soluble in THF at room temperature and stable when exposed to the atmosphere for a short period of time.)

For the retro-Diels–Alder reaction, each isomer of (OMN·MA)Cr(CO)$_3$ was refluxed in benzene under N_2, covering the oil bath system with foil to minimize exposure to light. Product analysis was carried out by HPLC at various time intervals up to 74 h.

B. Noncomplexed Ligands. No special precautions were used to avoid contact of the substrates with oxygen. A typical Diels–Alder reaction was as follows. Octamethylnaphthalene (36.1 mg, 0.15 mmol) and maleic anhydride (73.6 mg, 0.75 mmol) were refluxed in 1.0 mL of benzene and analyzed by HPLC (in 1.0 mL of THF as with the chromium complexes above) at various time intervals up to 66 h.

A typical retro-Diels–Alder reaction was as follows. OMN·MA (single isomer, 10.0 mg, 0.030 mmol) and maleic anhydride (11.6 mg, 0.12 mmol) were refluxed in 1.0 mL of benzene and analyzed by HPLC at various intervals up to 116 h.

Collection and Reduction of the X-ray Data. Suitable red crystals of (OMN)Cr(CO)$_3$ (A) grown from solutions of benzene and hexane were mounted on a glass fiber. Yellow crystals of (OMN·MA)Cr(CO)$_3$ (B) were grown in CH_2Cl_2/hexane mixtures. A suitable crystal was mounted inside a N_2-filled capillary since slow decomposition occurred in the presence of both air and light. The crystals were centered and indexed by the Enraf-Nonius CAD4-SDP peak search, centering, and indexing programs.[21] The

Scheme I

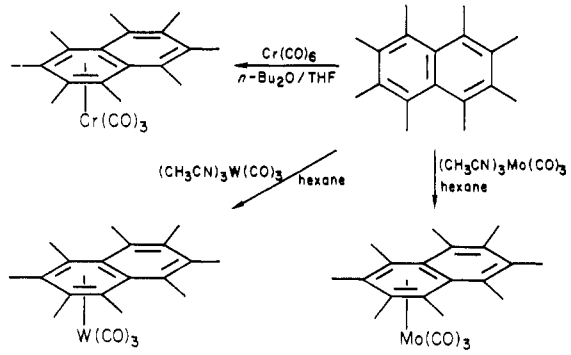

crystal systems were determined as triclinic for A and monoclinic for B. The centrosymmetric space group $P\bar{1}$ was chosen for A and eventually verified by successful refinement of the structure. The systematic absences in B uniquely identified the space group as $P2_1/c$. Summaries of the crystal data are presented in Tables I and II. Background counts were measured at both ends of the scan range by using a ω–2θ scan, equal at each side to one-fourth of the scan range of the peak. In this manner, the total duration of measured background is equal to half of the time required for the peak scan. The three check reflections in both A and B showed no decay during the course of data collection. In both structures the data intensity cutoff was set at $I > 2.5\sigma I$, which led to a total of 2665 reflections of A and 2013 reflections for B.[22] These were corrected for Lorrentz, polarization, and background effects but not for absorption.

Solution and Refinement of the Structure. The structures were solved by conventional heavy-atom techniques. The chromium atoms were located by a Patterson synthesis. Subsequent structure factor and difference Fourier calculations revealed the positions of the remaining nonhydrogen atoms.[23] After several

(21) All calculations were carried out on PDP 8A and 11/34 computers using the Enraf-Nonius CAD 4-SDP programs. This crystallographic computing package is described in: Frenz, B. A. In "Computing in Crystallography"; Schenk, H., Olthof-Hazekamp, R., van Koningsveld, H., Bassi, G. C., Eds.; Delft University Press: Delft, Holland, 1978; pp 64–71. Also "CAD 4 and SDP Users Manual"; Enraf-Nonius: Delft, Holland, 1978.

(22) The intensity data were processed as described: "CAD 4 and SDP Users Manual"; Enraf-Nonius: Delft, Holland, 1978. The net intensity $I = (K/\mathrm{NPI})(C - 2B)$, where $K = 20.1166x$ (attenuator factor); NPI = ratio of fastest possible scan rate to scan rate for the measurement, C = total count, and B = total background count. The standard deviation in the net intensity is given by $\mu^2(I) = (K/\mathrm{NPI})^2[C + 4B + (pI)^2]$, where p is a factor used to down weight intense reflections. The observed structure factor amplitude F_o is given by $F_o = (1/Lp)^{1/2}$, where Lp = Lorentz and polarization factors. The $\sigma(I)$'s were converted to the estimated errors in the relative structure factors $\sigma(F_o)$ and $\sigma(F_o) = {}^1/_2(\sigma(I)/I)F_o$.

(23) The function minimized was $\sum w(|F_o| - |F_c|)^2$, where $w = 1/\sigma^2(F_o)$. The unweighted and weighted residuals are defined as $R = (\sum||F_o| - |F_c||)/\sum|F_o|$ and $R_w = [(\sum w(|F_o| - |F_c|))^2/(\sum w|F_o|)^2]^{1/2}$. The error in an observation of unit weight is $[\sum w(|F_o| - |F_c|)^2/(\mathrm{NO} - \mathrm{NV}))]^{1/2}$, where NO and NV are the number of observations and variables, respectively.

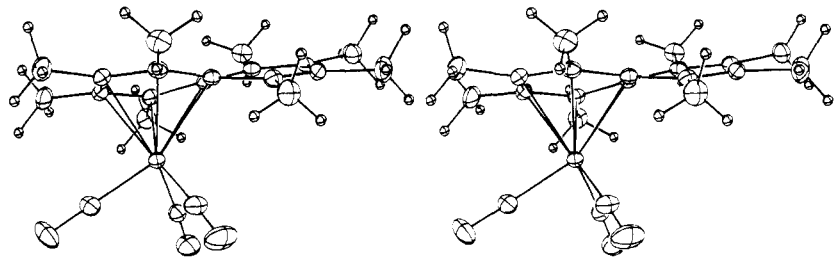

Figure 1. Stereoview of $(OMN)Cr(CO)_3$.

cycles of full-matrix least-squares refinement the difference Fourier calculations revealed the positions of every hydrogen atom in A and many of them in B. The remaining hydrogen atom positions in B could be calculated by using 1.0 Å for the C–H bond distance and $B(H) = B(C) + 1.0$ for the isotropic temperature factor. In the final least squares cycles the hydrogen atom parameters were not refined for B. However, in A both the position and isotropic temperature factors of every hydrogen were refined and were observed to converge normally. The values of the atomic scattering factors used in the calculations were taken from the usual tabulation,[24] and the effects of anomalous dispersion were included for the nonhydrogen atoms. The hydrogen atom scattering factors were taken from Cromer and Ibers' list.[25] Tables III and IV list the final positional and thermal parameters for the structures.

Results

Synthesis of $M(CO)_3$ Complexes. Scheme I shows the routes to the group 6 metal tricarbonyl complexes of OMN. The reactions proceed in moderate yields, with the exception of tungsten. These arene complexes are highly crystalline and relatively stable to air in the solid state but decompose in solution in the presence of oxygen. The order of air stability in solution is Cr > W > Mo, with the Cr complex stable over a period of hours and the Mo complex decomposing within minutes in the absence of an inert atmosphere. The spectroscopic properties of these and of all the compounds studied are given in Table V. The ^1H NMR spectra of the OMN complexes deserve comment. Although these structures are unsymmetric and should give rise to eight resonances, only four are observed. This is evidence that OMN is undergoing rapid ring flipping as shown.

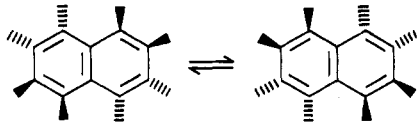

This result is not at all surprising, but it does experimentally confirm that octamethylnaphthalene can undergo this type of fluxional process. Due to the higher symmetry of OMN itself this rearrangement is undetectable. Attempts to "freeze" the motion of the complexes were not successful even at −100 °C by using a 270-MHz spectrometer. The variable-temperature work did show a substantial temperature dependence of the chemical shifts of every OMN complex.

Description of the Structure of $(OMN)Cr(CO)_3$. Figure 1 is a stereoview showing the overall structure of $(OMN)Cr(CO)_3$. The OMN ligand is bound to the $Cr(CO)_3$ group in the expected η^6 fashion. The structure of the OMN ligand is the same as that in its uncomplexed form,[15] which corresponds to the chiral point group D_2. The labeling is shown in Figure 2.

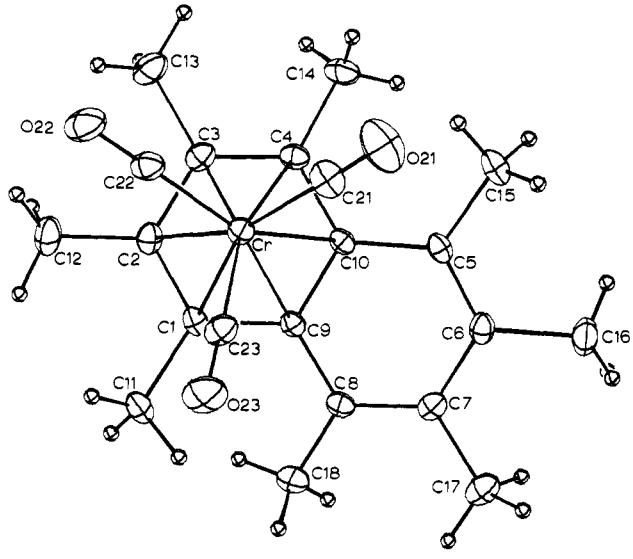

Figure 2. Atom labels for $(OMN)Cr(CO)_3$.

Due to the repulsive interactions principally involving the peri-methyl groups, the naphthalene ring system is severely distorted. These distortions are reflected in the bond distances and angles both within the ring and involving the methyls as well. One of the largest single effects of the distortions involves the expansion of the C1/4–C9/10–C8/5 angle to an average of 123.8 (2)°. The internal angles about C9/10 split the difference caused by this increase and average 118.1 (5)°. The remaining internal angles in the ring show no effect of the distortion and average 120.3 (7)°. The central C9–C10 bond distance is elongated to 1.440 (2) Å compared to 1.416 Å in OMN. As mentioned below this difference can be attributed to the metal. The C9/10/10/9–C1/4/5/8–C11/14/15/18 angles increase with the overall average being 121.0 (5)°. The distortions within these molecules are often best described by the various torsion angles. The twist about the C9–C10 bond is 19.3°, as measured by comparing the planes containing C1–C9–C10–C8 and C4–C9–C10–C5. The torsion angles C11/18/14/15–C1/8/4/5–C9/9/10/10–C8/1/5/4 average to 20 (1)° which reflects the additional distortion of the peri-methyl groups further out of the plane. A summary of distances and angles is given in Tables VI and VII.

We were able to locate and refine the positions and isotropic temperature factors of each of the methyl hydrogens. This now allows us to consider the orientation of the methyls as well as to probe the H–H interactions which are indeed causing the distortions. Both sets of peri-methyl groups are oriented as schematically shown in V. This orientation is similar to that of the methyl groups found in the 1,8-bis(trimethylstannyl)- and 1,8-bis(trimethylgermanyl)naphthalene[5] but differs from that observed in the *tert*-butyl derivative which exhibits the

(24) Cromer, D. T.; Waber, J. T. "International Tables for X-ray Crystallography"; Kynoch Press: Birmingham, England, 1974; Vol. IV, Table 2.2.4. Cromer, D. T. *Ibid.* Table 2.3.1.
(25) Cromer, D. T.; Ibers, J. A., in ref 24.

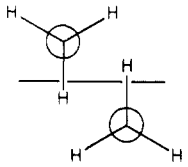

V

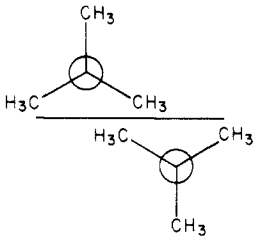

VI

idealized geometry,[3] VI. It would appear that in the less crowded compounds the former geometry is preferred.

Further examination shows that between the peri-methyl groups, two H–H contacts per methyl group are less than the van der Waals contact (~2.5 Å). As far as the remaining methyl groups, there is one short contact between each.

The distances each atom is displaced from the mean plane consisting of C1 through C10 are shown in Figure 3. This, along with the facts mentioned above, indicates that the $Cr(CO)_3$ group has no effect on the mode of distortion and only a small effect on the magnitude of these distortions. The most notable effects are the increases of the bond distances C1–C2, C3–C4, and C9–C10. These, of course, are the carbon–carbon bonds containing the most double-bond character. The increase averages about 0.03 Å compared to OMN itself, which is similar to the increase observed in (naphthalene)$Cr(CO)_3$,[26] and can be attributed to the filled metal π-type orbitals interacting with empty π^* orbitals.

A consideration of the Cr–C(arene) interaction shows a set of five distances with an average of 2.25 (2) Å. The Cr–C9 distance is exceptionally long at 2.406 (2) Å. (Naphthalene)$Cr(CO)_3$ also shows two sets of bond distances, however, they are symmetric with respect to the mirror plane. The Cr–C9 and Cr–C10 values average 2.32 (2) Å, while the remaining four bonds are 2.20 (1) Å. This phenomenon appears to be a general structural feature for $Cr(CO)_3$ complexes of polynuclear aromatics.[27] The difference observed in (OMN)$Cr(CO)_3$ appears because the twist of the molecule forces C10 closer to the chromium. Another way of considering the chromium–arene interaction is as being partway between a planar arene system and a cyclohexadienyl complex. In $(\eta_5\text{-}C_6H_7)Mn(CO)_3$ (VII),

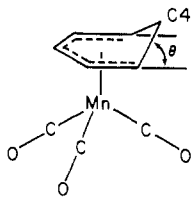

VII

the Mn–C4 bond distance is 2.76 Å.[28] Using the Cr–C9 distance of 2.409 (2) Å and the average of 2.25 (2) Å for the remaining five Cr–C distances, (OMN)$Cr(CO)_3$ is approximately one-third of the way toward a cyclohexadienyl system. Another measure of this is the angle θ which is 42° in the Mn compound and 38.6° in $\{(\eta^5\text{-}[(C_4H_7S_2)C_6H_6]Cr(CO)_3\}^-$.[29] In (OMN)$Cr(CO)_3$ the dihedral angle between the average plane comprised of C1–C2–C3–C4–C10 and C1–C9–C10 is 17.5°.

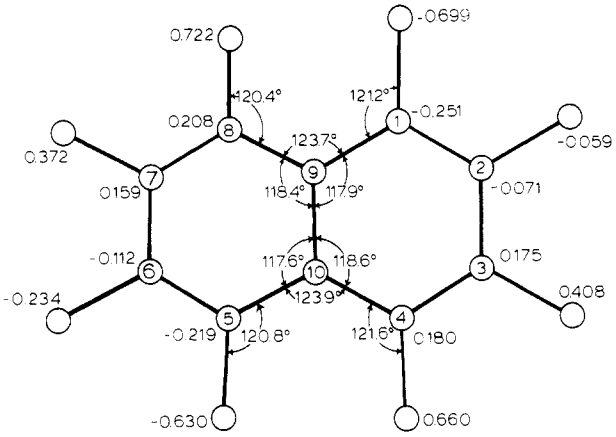

Figure 3. View of OMN ligand illustrating some of the effects of the molecular distortions. The fractional value beside each carbon is the distance below (+) or above (–) the average plane described by the ring carbons (C1–C10). The Cr atom is located above the C1-containing ring. The values for C9 and C10 are –0.031 and –0.033, respectively.

Description of the Structure of (*exo*-OMN·Ma)-$Cr(CO)_3$. A stereoview with selected labels is shown in Figure 4. The aromatic ring in the structure is planar and binds the $Cr(CO)_3$ group. The carbon–carbon bond distances around the ring are normal for (arene)tricarbonylchromium species. The average is 1.42 (2) Å, however, two of these, C9–C1 and C4–C10, are slightly longer at 1.445 (5) and 1.439 (5) Å, respectively. This could result from the crowding discussed below or possibly because C9 and C10 are involved in a bicyclic ring system. The $Cr(CO)_3$ is located symmetrically below the aromatic ring. The carbonyls, oriented in a staggered configuration, exhibit normal metal–carbon and carbon–oxygen parameters. The six Cr–C(arene) bonds are essentially equal and average 2.23 (2) Å.

The interesting feature of the structure centers around the distortions caused by the crowding between the methyl groups C18–C11 and C14–C15. Carbons C5 and C8 are now the two bridgehead atoms in the bicyclooctadiene ring system. The methyls (C15 and C18) are clearly tilted away from the aromatic ring methyls. This is easily seen by comparing the angles C9–C8–C18 and C10–C5–C15 which are 120.3 (3)° and 119.9 (4)°, respectively, with the angles C7–C8–C18 and C6–C5–C15 of 112.6 (4)° and 110.9 (4)°. The aromatic methyl groups in the 1- and 4-positions also reflect this crowding, as measured by the angles C9–C1–C11 or 122.8 (4)° and C10–C4–C14 of 123.4 (4)°. It is interesting that in this structure, however, the distortions are of the in-plane type. Specific distances and angles are presented in Tables VIII and IX.

Metal-Centered Reactivity of (OMN)$Cr(CO)_3$. The reactions of (OMN)$Cr(CO)_3$ with group 5 donors is dependent on the conditions. When dissolved in trimethyl phosphite and warmed to 70 °C for 2.0 h, complete displacement of OMN occurred (eq 1). Photolysis of

$$(OMN)Cr(CO)_3 + P(OCH_3)_3(\text{excess}) \xrightarrow[2.0\ h]{70\ °C} OMN + [P(OCH)_3]_3Cr(CO)_3 \quad (1)$$

(OMN)$Cr(CO)_3$ leads, however, to a different product. Purple crystals of (OMN)$Cr(CO)_2(PPh_3)$ can be obtained in reasonable yield by Pyrex-filtered UV irradiation of a hexane solution of (OMN)$Cr(CO)_3$ and PPh_3 (eq 2)

$$(OMN)Cr(CO)_3 + PPh_3 \xrightarrow{h\nu} CO + (OMN)Cr(CO)_2PPh_3 \quad (2)$$

(26) Kunz, V.; Nowacki, W. *Helv. Chim. Acta* **1967**, *50*, 1052.
(27) Cais, M.; Kaftory, M.; Kohn, D. H.; Tatrasky, D. *J. Organomet. Chem.* **1979**, *184*, 103.
(28) Churchhill, M. R.; Scholer, F. R. *Inorg. Chem.* **1969**, *8*, 1950.
(29) Semmelhack, M. F.; Hall, H. T., Jr.; Farina, R.; Yoshifuji, M.; Clark, G.; Bargar, T.; Hirotsu, K.; Clardy, J. *J. Am. Chem. Soc.* **1979**, *101*, 3535.

Table III. Positional and Thermal Parameters and Their Estimated Standard Deviations for $(OMN)Cr(CO)_3$[a]

atom	x	y	z	B(1,1)	B(2,2)	B(3,3)	B(1,2)	B(1,3)	B(2,3)
Cr	0.17527 (3)	0.18144 (2)	0.31747 (4)	0.01066 (3)	0.00393 (1)	0.01146 (4)	−0.00225 (4)	0.00809 (6)	0.00034 (4)
O21	−0.0875 (2)	0.1487 (2)	0.4138 (3)	0.0217 (2)	0.01500 (16)	0.0346 (3)	−0.0100 (3)	0.0318 (4)	0.0109 (4)
O22	0.3233 (2)	−0.0317 (1)	0.3949 (3)	0.0257 (3)	0.00414 (8)	0.0274 (4)	−0.0040 (3)	0.0034 (6)	0.0011 (3)
O23	0.3679 (2)	0.2117 (1)	0.7229 (2)	0.0265 (3)	0.00846 (11)	0.0125 (3)	−0.0060 (3)	0.0061 (5)	−0.0022 (3)
C21	0.0116 (3)	0.1629 (2)	0.3741 (3)	0.0152 (3)	0.00743 (13)	0.0174 (3)	−0.0045 (3)	0.0127 (5)	0.0042 (4)
C22	0.2643 (2)	0.0508 (1)	0.3654 (3)	0.0153 (3)	0.00482 (10)	0.0146 (3)	−0.0050 (3)	0.0058 (5)	−0.0008 (3)
C23	0.2913 (2)	0.2016 (1)	0.5659 (3)	0.0164 (3)	0.00442 (10)	0.0155 (3)	−0.0030 (3)	0.0125 (4)	−0.0001 (3)
C4	0.0171 (2)	0.2176 (1)	0.0119 (2)	0.0122 (2)	0.00436 (9)	0.0118 (3)	−0.0048 (2)	0.0064 (4)	0.0006 (3)
C3	0.1645 (2)	0.1568 (1)	0.0260 (2)	0.0157 (3)	0.00439 (10)	0.0123 (3)	−0.0026 (3)	0.0123 (4)	−0.0008 (3)
C2	0.3160 (2)	0.1810 (1)	0.1492 (2)	0.0124 (2)	0.00507 (10)	0.0136 (3)	−0.0005 (3)	0.0135 (4)	0.0009 (3)
C1	0.3169 (2)	0.2684 (1)	0.2507 (2)	0.0088 (2)	0.00512 (10)	0.0130 (3)	−0.0024 (2)	0.0089 (3)	0.0014 (3)
C9	0.1663 (2)	0.3402 (1)	0.2155 (2)	0.0086 (2)	0.00447 (9)	0.0100 (2)	−0.0029 (2)	0.0065 (3)	0.0007 (3)
C8	0.1589 (2)	0.4423 (1)	0.2686 (2)	0.0112 (2)	0.00449 (9)	0.0108 (3)	−0.0042 (2)	0.0061 (4)	0.0007 (3)
C7	0.0160 (2)	0.5010 (1)	0.2621 (2)	0.0142 (3)	0.00409 (9)	0.0107 (3)	−0.0016 (3)	0.0083 (4)	0.0011 (3)
C6	−0.1256 (2)	0.4619 (1)	0.2011 (2)	0.0104 (2)	0.00526 (11)	0.0128 (3)	0.0012 (3)	0.0083 (4)	0.0020 (3)
C5	−0.1279 (2)	0.3686 (1)	0.1332 (2)	0.0082 (2)	0.00547 (10)	0.0130 (3)	−0.0020 (2)	0.0058 (4)	0.0022 (3)
C10	0.0166 (2)	0.3076 (1)	0.1196 (2)	0.0090 (2)	0.00423 (9)	0.0103 (3)	−0.0031 (2)	0.0052 (3)	0.0012 (3)
C14	−0.1368 (3)	0.1961 (2)	−0.1421 (3)	0.0162 (3)	0.00620 (12)	0.0169 (4)	−0.0089 (3)	0.0038 (6)	−0.0029 (4)
C13	0.1657 (3)	0.0634 (2)	−0.0871 (3)	0.0237 (4)	0.00555 (12)	0.0189 (4)	−0.0033 (4)	0.0176 (6)	−0.0058 (4)
C12	0.4727 (3)	0.1140 (2)	0.1597 (3)	0.0163 (3)	0.00745 (15)	0.0226 (4)	0.0033 (4)	0.0218 (5)	−0.0011 (4)
C11	0.4781 (2)	0.2858 (2)	0.4001 (3)	0.0089 (2)	0.00706 (13)	0.0199 (4)	−0.0034 (3)	0.0077 (5)	0.0008 (4)
C18	0.2993 (2)	0.4895 (2)	0.3026 (3)	0.0148 (3)	0.00561 (11)	0.0196 (4)	−0.0083 (3)	0.0104 (5)	−0.0004 (3)
C17	0.0067 (3)	0.6077 (2)	0.3220 (3)	0.0219 (4)	0.00442 (11)	0.0212 (4)	−0.0019 (3)	0.0173 (6)	−0.0009 (4)
C16	−0.2775 (3)	0.5292 (2)	0.2082 (3)	0.0128 (3)	0.00811 (17)	0.0238 (5)	0.0035 (4)	0.0131 (6)	−0.0030 (5)
C15	−0.2771 (2)	0.3274 (2)	0.0863 (3)	0.0097 (2)	0.00798 (15)	0.0265 (4)	−0.0047 (3)	0.0136 (5)	0.0009 (4)

atom	x	y	z	B, Å	atom	x	y	z	B, Å
H14A	−0.110 (2)	0.170 (2)	−0.241 (3)	4.5 (5)	H18A	0.368 (2)	0.451 (2)	0.246 (3)	4.2 (5)
H14B	−0.176 (3)	0.158 (2)	−0.111 (3)	5.5 (6)	H18B	0.367 (2)	0.494 (2)	0.432 (3)	4.5 (5)
H14C	−0.219 (3)	0.253 (2)	−0.188 (3)	5.7 (6)	H18C	0.259 (3)	0.553 (2)	0.249 (3)	4.9 (5)
H13A	0.170 (3)	0.075 (2)	−0.200 (4)	6.8 (7)	H17A	−0.031 (3)	0.618 (2)	0.426 (4)	7.5 (8)
H13B	0.247 (3)	0.011 (2)	−0.012 (3)	6.6 (7)	H17B	−0.073 (3)	0.651 (2)	0.222 (3)	6.7 (7)
H13C	0.065 (3)	0.038 (2)	−0.135 (4)	7.6 (8)	H17C	0.106 (3)	0.630 (2)	0.374 (4)	7.6 (8)
H12A	0.569 (4)	0.133 (2)	0.257 (4)	8.9 (9)	H16A	−0.356 (5)	0.499 (3)	0.153 (5)	12.3 (12)
H12B	0.474 (3)	0.100 (2)	0.055 (4)	8.0 (8)	H16B	−0.275 (3)	0.551 (2)	0.326 (3)	6.4 (7)
H12C	0.485 (3)	0.042 (2)	0.206 (4)	6.9 (7)	H16C	−0.297 (3)	0.603 (2)	0.146 (4)	7.4 (8)
H11A	0.460 (2)	0.331 (1)	0.505 (3)	3.9 (5)	H15A	−0.251 (2)	0.257 (1)	0.094 (3)	3.8 (5)
H11B	0.548 (3)	0.312 (2)	0.349 (3)	5.8 (6)	H15B	−0.364 (3)	0.350 (2)	−0.035 (3)	4.9 (6)
H11C	0.540 (2)	0.225 (2)	0.468 (3)	4.8 (5)	H15C	−0.318 (3)	0.345 (2)	0.169 (3)	5.0 (5)

[a] The form of the anisotropic thermal parameter is $\exp[-(B(1,1)h^2 + B(2,2)k^2 + B(3,3)l^2 + B(1,2)hk + B(1,3)hl + B(2,3)kl)]$.

Table IV. Positional and Thermal Parameters and Their Estimated Standard Deviations for (OMN·MA)Cr(CO)$_3$[a]

atom	x	y	z	B(1,1)	B(2,2)	B(3,3)	B(1,2)	B(1,3)	B(2,3)
Cr	0.26705 (5)	0.05532 (9)	0.04080 (4)	0.00329 (3)	0.00776 (9)	0.00303 (2)	0.0002 (1)	0.00323 (3)	−0.0016 (1)
O19	0.2410 (2)	−0.0841 (4)	−0.2901 (2)	0.0104 (2)	0.0142 (6)	0.0047 (1)	−0.0020 (6)	0.0096 (2)	0.0026 (5)
O20	0.3219 (2)	−0.2541 (4)	−0.1904 (2)	0.0047 (1)	0.0128 (5)	0.0045 (1)	−0.0046 (5)	0.0058 (2)	−0.0027 (5)
O22	0.3674 (2)	−0.4426 (4)	−0.0971 (2)	0.0054 (2)	0.0136 (6)	0.0087 (2)	0.0055 (6)	0.0081 (2)	0.0038 (7)
O23	0.0964 (2)	0.2388 (4)	−0.0492 (2)	0.0059 (2)	0.0144 (6)	0.0089 (2)	0.0091 (6)	0.0075 (3)	0.0040 (6)
O24	0.3547 (3)	0.2783 (5)	0.1851 (3)	0.0089 (3)	0.0302 (8)	0.0100 (2)	−0.0056 (8)	0.0063 (4)	−0.0256 (7)
O25	0.1863 (2)	−0.0735 (5)	0.1512 (2)	0.0104 (2)	0.0200 (7)	0.0090 (2)	0.0131 (6)	0.0154 (2)	0.0143 (6)
C1	0.3597 (3)	−0.1335 (5)	0.0574 (2)	0.0030 (2)	0.0083 (7)	0.0025 (2)	0.0012 (6)	0.0028 (2)	−0.0000 (6)
C2	0.4100 (3)	−0.0068 (5)	0.0642 (3)	0.0025 (2)	0.0088 (7)	0.0031 (2)	−0.0007 (6)	0.0026 (3)	−0.0023 (6)
C3	0.3753 (3)	0.0994 (5)	−0.0045 (3)	0.0028 (2)	0.0073 (7)	0.0033 (2)	−0.0004 (6)	0.0030 (2)	−0.0012 (6)
C4	0.2862 (3)	0.0826 (5)	−0.0810 (3)	0.0036 (2)	0.0072 (7)	0.0035 (2)	0.0004 (6)	0.0040 (2)	−0.0007 (6)
C5	0.1386 (3)	−0.0914 (5)	−0.1717 (3)	0.0034 (2)	0.0076 (7)	0.0023 (2)	0.0005 (7)	0.0005 (3)	−0.0006 (6)
C6	0.0774 (3)	−0.1564 (6)	−0.1336 (3)	0.0025 (2)	0.0100 (7)	0.0041 (2)	0.0003 (7)	0.0020 (3)	−0.0032 (7)
C7	0.1155 (3)	−0.2628 (5)	−0.0742 (3)	0.0038 (2)	0.0100 (7)	0.0036 (2)	−0.0033 (7)	0.0042 (3)	−0.0044 (6)
C8	0.2160 (3)	−0.2992 (5)	−0.0518 (3)	0.0032 (2)	0.0073 (6)	0.0024 (2)	−0.0007 (6)	0.0028 (2)	−0.0006 (6)
C9	0.2721 (3)	−0.1559 (5)	−0.0238 (2)	0.0029 (2)	0.0060 (6)	0.0019 (1)	−0.0002 (6)	0.0027 (2)	−0.0014 (5)
C10	0.2337 (2)	−0.0467 (5)	−0.0896 (2)	0.0025 (2)	0.0064 (6)	0.0023 (1)	0.0002 (7)	0.0020 (2)	−0.0001 (6)
C11	0.3987 (3)	−0.2394 (6)	0.1347 (3)	0.0048 (3)	0.0119 (8)	0.0033 (2)	−0.0018 (8)	0.0012 (4)	0.0025 (7)
C12	0.5051 (3)	0.0174 (6)	0.1457 (3)	0.0041 (2)	0.0122 (9)	0.0043 (2)	−0.0022 (8)	0.0016 (4)	−0.0012 (8)
C13	0.4344 (3)	0.2294 (6)	0.0044 (3)	0.0043 (2)	0.0079 (7)	0.0065 (3)	−0.0018 (8)	0.0041 (4)	−0.0001 (8)
C14	0.2518 (3)	0.2028 (6)	−0.1510 (3)	0.0058 (3)	0.0084 (7)	0.0045 (2)	−0.0009 (8)	0.0037 (4)	0.0033 (7)
C15	0.0834 (3)	0.0178 (6)	−0.2465 (3)	0.0048 (3)	0.0108 (9)	0.0044 (3)	0.0020 (8)	−0.0001 (4)	0.0028 (8)
C16	−0.0180 (3)	−0.0957 (6)	−0.1601 (4)	0.0041 (2)	0.0132 (10)	0.0092 (3)	0.0010 (8)	0.0058 (4)	−0.0017 (9)
C17	0.0700 (3)	−0.3418 (7)	−0.0271 (3)	0.0053 (2)	0.0162 (9)	0.0055 (2)	−0.0064 (8)	0.0072 (3)	−0.0032 (8)
C18	0.2531 (3)	−0.4332 (6)	0.0080 (3)	0.0063 (2)	0.0068 (6)	0.0046 (2)	−0.0024 (8)	0.0052 (3)	0.0002 (7)
C19	0.2424 (3)	−0.1739 (6)	−0.2393 (3)	0.0056 (2)	0.0098 (7)	0.0023 (2)	−0.0024 (8)	0.0031 (3)	−0.0037 (6)
C20	0.1679 (3)	−0.2188 (5)	−0.2135 (3)	0.0035 (2)	0.0093 (7)	0.0025 (2)	−0.0009 (7)	0.0023 (3)	−0.0018 (6)
C21	0.2121 (3)	−0.3398 (5)	−0.1463 (3)	0.0034 (2)	0.0071 (6)	0.0031 (2)	−0.0032 (6)	0.0037 (2)	−0.0023 (6)
C22	0.3084 (3)	−0.3574 (5)	−0.1378 (3)	0.0047 (2)	0.0080 (7)	0.0041 (2)	−0.0019 (7)	0.0051 (3)	−0.0032 (6)
C23	0.1632 (3)	0.1673 (6)	−0.0122 (3)	0.0044 (2)	0.0089 (7)	0.0055 (2)	0.0010 (7)	0.0058 (3)	−0.0011 (7)
C24	0.3201 (3)	0.1918 (7)	0.1290 (3)	0.0050 (3)	0.0181 (10)	0.0052 (2)	−0.0024 (9)	0.0043 (4)	−0.0105 (8)
C25	0.2176 (3)	−0.0251 (6)	0.1077 (3)	0.0055 (2)	0.0117 (8)	0.0046 (2)	0.0068 (7)	0.0067 (3)	0.0050 (7)

atom	x	y	z	B, Å^2	atom	x	y	z	B, Å^2
H11A	0.4375 (0)	−0.1953 (0)	0.1875 (0)	4.8000 (0)	H15B	0.1245 (0)	0.0492 (0)	−0.2761 (0)	5.7000 (0)
H11B	0.3470 (0)	−0.2847 (0)	0.1442 (0)	4.8000 (0)	H15C	0.0270 (0)	−0.0301 (0)	−0.2956 (0)	5.7000 (0)
H11C	0.4346 (0)	−0.3183 (0)	0.1246 (0)	4.8000 (0)	H16A	−0.0523 (0)	−0.0852 (0)	−0.2284 (0)	5.6000 (0)
H12A	0.5625 (0)	0.0273 (0)	0.1250 (0)	4.9000 (0)	H16B	−0.0561 (0)	−0.1628 (0)	−0.1418 (0)	5.6000 (0)
H12B	0.5038 (0)	0.1067 (0)	0.1790 (0)	4.9000 (0)	H16C	−0.0153 (0)	0.0008 (0)	−0.1316 (0)	5.6000 (0)
H12C	0.5202 (0)	−0.0674 (0)	0.1889 (0)	4.9000 (0)	H17A	0.0000 (0)	−0.3320 (0)	−0.0625 (0)	4.2000 (0)
H13A	0.4570 (0)	0.2773 (0)	0.0625 (0)	4.3000 (0)	H17B	0.0862 (0)	−0.4461 (0)	−0.0202 (0)	4.2000 (0)
H13B	0.4911 (0)	0.2002 (0)	−0.0016 (0)	4.3000 (0)	H17C	0.0899 (0)	−0.2991 (0)	0.0351 (0)	4.2000 (0)
H13C	0.3978 (0)	0.3016 (0)	−0.0437 (0)	4.3000 (0)	H18A	0.2500 (0)	−0.4180 (0)	0.0625 (0)	4.0000 (0)
H14A	0.1875 (0)	0.2227 (0)	−0.1680 (0)	4.4000 (0)	H18B	0.2150 (0)	−0.5212 (0)	−0.0232 (0)	4.0000 (0)
H14B	0.2879 (0)	0.2956 (0)	−0.1259 (0)	4.4000 (0)	H18C	0.3202 (0)	−0.4533 (0)	0.0236 (0)	4.0000 (0)
H14C	0.2558 (0)	0.1773 (0)	−0.2074 (0)	4.4000 (0)	H20	0.1055 (0)	−0.2500 (0)	−0.2695 (0)	3.1000 (0)
H15A	0.0625 (0)	0.1113 (0)	−0.2305 (0)	5.7000 (0)	H21	0.1680 (0)	−0.4434 (0)	−0.1660 (0)	3.0000 (0)

[a] The form of the anisotropic thermal parameter is $\exp[-B(1,1)h^2 + B(2,2)k^2 + B(3,3)l^2 + B(1,2)hk + B(1,3)hl + B(2,3)kl)]$.

Table V. Spectroscopic Properties of OMN Derivatives

compd	color	ν_{CO}, cm^{-1}	^1H NMR δ^c	ref
$(OMN)Cr(CO)_3$	red	1956 s, 1891 m, 1876 m (hexane)	2.62 (6 H), 2.58 (6 H), 2.38 (6 H), 2.33 (6 H)	*a*
$(OMN)Mo(CO)_3$	yellow	1942 s, 1858 s (CH_2Cl_2)	2.60 (6 H), 2.54 (6 H), 2.43 (6 H), 2.31 (6 H)	*a*
$(OMN)W(CO)_3$	orange	1940 s, 1843 s (CH_2Cl_2)	2.70 (6 H), 2.54 (6 H), 2.51 (6 H), 2.32 (6 H)	*a*
$(OMN)Cr(CO)_2(PPh_3)$	purple	1855 s, 1791 m (CH_2Cl_2)	7.19 (m, 15 H), 2.36 (6 H), 2.22 (6 H), 2.20 (6 H) 2.12 (6 H)	*a*
(*endo*-OMN·MA)$Cr(CO)_3$	yellow	1955 (s), 1877 m, 1776 w (CH_2Cl_2)	3.06 (2 H), 2.53 (6 H), 2.22 (6 H), 2.18 (6 H), 1.83 (6 H)	*b*
(*exo*-OMN·MA)$Cr(CO)_3$	yellow	1955 (s), 1877 m, 1776 w (CH_2Cl_2)	3.02 (2 H), 2.43 (6 H), 2.21 (6 H), 2.18 (6 H), 1.88 (6 H)	*b*
endo-OMN·MA	white	1857 w, 1778 s (Nujol)	3.13 (2 H), 2.50 (6 H), 2.23 (6 H), 2.20 (6 H), 1.74 (6 H)	*b*
exo-OMN·MA	white	1857 w, 1770 s (Nujol)	2.97 (2 H), 2.40 (6 H), 2.25 (6 H), 2.15 (6 H), 1.77 (6 H)	*b*

[a] Spectrum obtained in CD_2Cl_2 at 270 MHz. [b] Spectrum obtained in $CDCl_3$ at 80 MHz. [c] All resonances are singlets unless otherwise noted.

Table VI. Interatomic Distances for $(OMN)Cr(CO)_3$

atoms	dis, Å	atoms	dis, Å
Cr-C21	1.840 (2)	C6-C16	1.525 (3)
Cr-C22	1.824 (2)	C7-C17	1.518 (3)
Cr-C23	1.833 (2)	C8-C18	1.516 (2)
Cr-C1	2.230 (2)	C11-H11A	1.04 (2)
Cr-C2	2.229 (2)	C11-H11B	1.04 (3)
Cr-C3	2.264 (2)	C11-H11C	0.97 (3)
Cr-C4	2.270 (2)	C12-H12A	0.98 (4)
Cr-C9	2.406 (2)	C12-H12B	0.84 (3)
Cr-C10	2.257 (2)	C12-H12C	1.07 (3)
C21-O21	1.156 (3)	C13-H13A	0.95 (3)
C22-O22	1.154 (2)	C13-H13B	0.96 (3)
C23-O23	1.158 (2)	C13-H13C	0.99 (3)
C1-C2	1.399 (3)	C14-H14A	0.93 (3)
C2-C3	1.435 (3)	C14-H14B	0.82 (3)
C3-C4	1.400 (3)	C14-H14C	0.95 (3)
C4-C10	1.452 (2)	C15-H15A	0.96 (2)
C9-C10	1.440 (2)	C15-H15B	0.98 (3)
C5-C6	1.365 (3)	C15-H15C	0.88 (3)
C6-C7	1.424 (3)	C16-H16A	0.87 (4)
C7-C8	1.374 (3)	C16-H16B	0.95 (3)
C8-C9	1.444 (2)	C16-H16C	1.13 (3)
C1-C9	1.455 (2)	C17-H17A	1.01 (3)
C5-C10	1.457 (2)	C17-H17B	0.96 (3)
C1-C11	1.527 (2)	C17-H17C	0.96 (3)
C2-C12	1.513 (3)	C18-H18A	0.97 (2)
C3-C13	1.513 (3)	C18-H18B	0.96 (3)
C4-C14	1.514 (2)	C18-H18C	0.94 (3)
C5-C15	1.519 (3)		

Table VII. Selected Bond Angles for $(OMN)Cr(CO)_3$

atoms	angle, deg	atoms	angle, deg
C21-Cr-C22	87.32 (9)	Cr-C21-O21	177.7 (2)
C21-Cr-C23	88.45 (9)	Cr-C22-O22	178.6 (2)
C22-Cr-C23	86.80 (8)	Cr-C23-O23	177.9 (2)
C21-Cr-C1	155.79 (9)	Cr-C1-C11	120.2 (1)
C21-Cr-C2	158.55 (8)	Cr-C2-C12	130.3 (1)
C21-Cr-C3	121.47 (8)	Cr-C3-C13	130.0 (2)
C21-Cr-C4	95.77 (8)	Cr-C4-C14	139.4 (2)
C21-Cr-C9	120.14 (8)	Cr-C9-C8	143.3 (1)
C21-Cr-C10	94.00 (8)	Cr-C10-C5	122.4 (1)
C22-Cr-C1	116.59 (8)	C1-C2-C3	119.7 (2)
C22-Cr-C2	89.19 (8)	C2-C3-C4	120.9 (2)
C22-Cr-C3	88.82 (8)	C3-C4-C10	119.9 (2)
C22-Cr-C4	114.03 (7)	C4-C10-C9	118.6 (2)
C22-Cr-C9	152.42 (8)	C4-C10-C5	123.9 (2)
C22-Cr-C10	151.44 (7)	C10-C9-C1	117.9 (2)
C23-Cr-C1	89.15 (7)	C10-C9-C8	118.4 (1)
C23-Cr-C2	112.49 (8)	C1-C9-C8	123.7 (1)
C23-Cr-C3	149.52 (8)	C9-C8-C7	120.0 (2)
C23-Cr-C4	158.86 (7)	C8-C7-C6	120.3 (2)
C23-Cr-C9	95.83 (7)	C7-C6-C5	121.6 (2)
C23-Cr-C10	121.74 (7)	C2-C1-C9	120.2 (2)
C1-Cr-C2	36.57 (7)	C6-C5-C10	119.7 (2)
C2-Cr-C3	37.24 (7)	C5-C10-C9	117.6 (2)
C3-Cr-C4	35.99 (7)	C9-C1-C11	121.2 (2)
C4-Cr-C10	37.42 (6)	C9-C8-C18	120.4 (2)
C10-Cr-C9	35.78 (5)	C2-C1-C11	118.6 (2)
C9-Cr-C1	36.33 (6)	C7-C8-C18	118.9 (2)
C1-C2-C12	120.8 (2)	C10-C4-C14	121.6 (2)
C3-C2-C12	119.4 (2)	C10-C5-C15	120.8 (2)
C2-C3-C13	119.0 (2)	C3-C4-C14	117.6 (2)
C4-C3-C13	120.1 (2)	C6-C5-C15	119.4 (2)
C7-C6-C16	117.6 (2)		
C5-C6-C16	120.8 (2)		
C6-C7-C17	118.9 (2)		
C8-C7-C17	120.8 (2)		

Octamethylnaphthalene-Centered Reactivity of $(OMN)Cr(CO)_3$. $(OMN)Cr(CO)_3$ was found to undergo a Diels–Alder reaction with maleic anhydride. The isomeric compounds were conveniently separated by fractional crystallization from benzene/hexane solutions or by chromatography.

Both yellow crystalline products were shown by elemental and mass spectral analyses to have the formula $C_{25}H_{26}CrO_6$. ^1H NMR and infrared spectral studies further illustrated the similarities but gave no conclusive information allowing the assignment of the stereochemistry. Consideration of the reaction itself would give four possible products, VIII–XI (Scheme II). An X-ray structural analysis of one of the isomers proved that it had the stereochemistry illustrated by VIII. Decomplexation of the chromium from the ligand for each complex by photolysis under O_2 yielded the two separate isomers of OMN·MA. This result allows us to immediately eliminate X from consideration. We have no absolute proof which would allow differentiation between IX and XI as the second isomer, but the well-established steric directing effect of the $Cr(CO)_3$[20] makes attack of maleic anhydride from the opposite side of the OMN the only reasonable route. Therefore IX is assigned to the structure of the second isomer.

The Diels–Alder reaction of OMN itself was first reported in 1953.[11] The separation and assignment of the individual isomers was later made by Oku and co-workers[30] and was based on predicted shifts of the methine hydrogen. Our data show that the original stereochemical assignment of the OMN·MA isomers are reversed. From the X-ray structural analysis of (*exo*-OMN·MA)$Cr(CO)_3$ we know the stereochemistry. The oxidative removal of the Cr gives only one product which is the *exo*-OMN·MA having δ 2.97. Corresponding decomplexation of the (*endo*-OMN·MA)-$Cr(CO)_3$ gives only the endo product with δ 3.13.

(30) Oku, A.; Ohnishi, Y.; Mashio, F. *J. Org. Chem.* 1972, *37*, 4264.

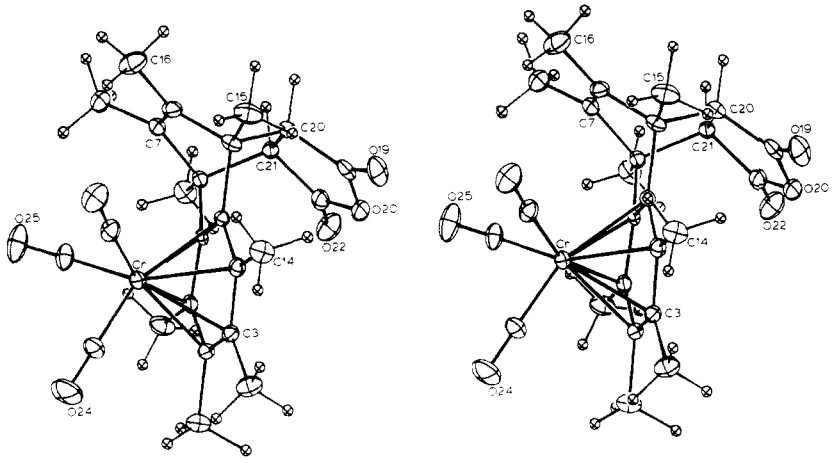

Figure 4. Stereoview and partial atom labels for (*exo*-OMN·MA)Cr(CO)$_3$. The basic OMN framework is numbered the same way as is (OMN)Cr(CO)$_3$. The anhydride portion consists of C19 through C22. This numbering sequence was adopted for simplicity in comparing the two structures and bears no resemblance to the usual nomenclature numbering sequence.

Table VIII. Bond Distances for (*exo*-OMN·MA)Cr(CO)$_3$

atoms	dist, Å	atoms	dist, Å
Cr-C23	1.816 (5)	C7-C6	1.329 (6)
Cr-C24	1.824 (5)	C6-C5	1.534 (5)
Cr-C25	1.816 (5)	C5-C10	1.563 (5)
Cr-C1	2.240 (4)	C8-C21	1.595 (5)
Cr-C2	2.238 (4)	C21-C20	1.511 (6)
Cr-C3	2.253 (4)	C21-C22	1.510 (6)
Cr-C4	2.214 (4)	C22-O22	1.179 (5)
Cr-C9	2.258 (4)	C22-O20	1.386 (5)
Cr-C10	2.199 (4)	O20-C19	1.376 (5)
C23-O23	1.168 (5)	C19-O19	1.183 (5)
C24-O24	1.159 (5)	C19-C20	1.519 (6)
C25-O25	1.156 (5)	C20-C5	1.558 (5)
C1-C2	1.405 (5)	C1-C11	1.506 (5)
C2-C3	1.414 (5)	C2-C12	1.520 (6)
C3-C4	1.418 (5)	C3-C13	1.504 (5)
C4-C10	1.439 (5)	C4-C14	1.520 (5)
C10-C9	1.408 (5)	C5-C15	1.529 (6)
C9-C1	1.445 (5)	C6-C16	1.503 (6)
C9-C8	1.554 (5)	C7-C17	1.500 (6)
C8-C7	1.529 (5)	C8-C18	1.531 (6)

Table IX. Bond Angles for (*exo*-OMN·MA)Cr(CO)$_3$

atoms	angle, deg	atoms	angle, deg
C23-Cr-C24	88.5 (2)	Cr-C1-C11	127.1 (3)
C23-Cr-C25	87.6 (2)	Cr-C2-C12	130.5 (3)
C24-Cr-C25	88.0 (2)	Cr-C3-C13	132.3 (3)
C23-Cr-C1	157.3 (2)	Cr-C4-C14	129.2 (3)
C23-Cr-C2	151.6 (2)	Cr-C9-C8	137.7 (3)
C23-Cr-C3	115.0 (2)	Cr-C10-C5	131.7 (3)
C23-Cr-C4	89.1 (2)	C2-C1-C9	118.2 (4)
C23-Cr-C9	119.8 (2)	C2-C1-C11	118.9 (4)
C23-Cr-C10	91.4 (2)	C9-C1-C11	122.8 (4)
C24-Cr-C1	114.2 (2)	C1-C2-C3	121.6 (4)
C24-Cr-C2	89.0 (2)	C1-C2-C12	120.2 (4)
C24-Cr-C3	90.0 (2)	C3-C2-C12	118.2 (4)
C24-Cr-C4	116.6 (2)	C2-C3-C4	120.2 (4)
C24-Cr-C9	151.7 (2)	C2-C3-C13	119.2 (4)
C24-Cr-C10	154.6 (2)	C4-C3-C13	120.6 (4)
C25-Cr-C1	93.6 (2)	C3-C4-C10	119.1 (4)
C25-Cr-C2	120.5 (2)	C3-C4-C14	117.5 (4)
C25-Cr-C3	157.2 (2)	C10-C4-C14	123.4 (4)
C25-Cr-C4	155.2 (2)	C5-C10-C9	112.7 (4)
C25-Cr-C9	93.6 (2)	C4-C10-C5	127.0 (4)
C25-Cr-C10	117.4 (2)	C4-C10-C9	120.0 (3)
C1-Cr-C2	36.6 (1)	C1-C9-C8	125.7 (4)
C2-Cr-C3	36.7 (1)	C10-C9-C1	120.6 (4)
C3-Cr-C4	37.0 (1)	C10-C9-C8	113.5 (3)
C4-Cr-C10	38.1 (1)	C10-C5-C15	119.9 (4)
C10-Cr-C9	36.8 (1)	C10-C5-C6	107.7 (3)
C9-Cr-C1	37.5 (1)	C10-C5-C20	102.2 (3)
Cr-C23-O23	177.6 (4)	C6-C5-C15	110.9 (4)
Cr-C24-O24	179.3 (5)	C6-C5-C20	106.4 (3)
Cr-C25-O25	178.5 (5)	C15-C5-C20	108.7 (3)
C7-C6-C16	123.5 (4)	C5-C6-C16	120.5 (4)
C6-C7-C17	125.7 (4)	C5-C6-C7	115.9 (4)
C6-C7-C8	114.6 (4)	C20-C21-C22	104.9 (3)
C8-C7-C17	119.7 (4)	C21-C22-O20	109.3 (4)
C7-C8-C18	112.6 (4)	C21-C22-O22	130.5 (5)
C7-C8-C9	106.9 (3)	O20-C22-O22	120.2 (4)
C7-C8-C21	105.6 (3)	C22-O20-C19	111.6 (4)
C9-C8-C18	120.3 (3)	O20-C19-O19	120.3 (5)
C9-C8-C21	104.3 (3)	O20-C19-C20	109.3 (4)
C18-C8-C21	106.0 (3)	O19-C19-C20	130.4 (5)
C8-C21-C20	110.2 (3)	C19-C20-C21	104.7 (4)
C8-C21-C22	112.0 (3)	C19-C20-C5	111.8 (4)
		C5-C20-C21	111.6 (3)

In order to obtain a more quantitative evaluation of the effect of the Cr(CO)$_3$ on the reactivity of OMN, we carefully monitored the reactions by using high-pressure liquid chromatography. The following two effects were explored. How does the rate of reaction differ? Further, does the Cr(CO)$_3$ change the equilibrium constant for the reaction?

After 66 h at 80 °C the estimates for the equilibrium are 6 and 1 for the exo and endo isomer, respectively. This is in reasonable agreement with previously reported measurement by Hart[31] and Oku and co-workers[30] (summarized in Table X). Although the exo isomer is thermodynamically favored, the less stable endo isomer is formed more rapidly in the initial stage of the reaction. The equilibrium composition is also approached from a mixture of either the endo or exo isomer and 4 equiv of maleic anhydride. Unfortunately, quantitative measurement of the retro-Diels–Alder reaction was prohibited by side reactions of the starting adducts apparently caused by the high initial concentrations of the adducts combined with the longer reaction times. This was a particularly difficult problem with the endo isomer.

Under identical conditions we found that (OMN)Cr(CO)$_3$ reacted with MA at approximately the same rate as OMN did. There was, however, a substantial difference in the equilibrium constants for the reaction. The average values obtained from duplicate experiments were K(exo) = 870 (average of 880 and 860) and K(endo) = 390 (average of 400 and 380). The equilibrium again was approached by starting with each isomer, but the reaction was so slow it could not be accurately determined due to the small amount of decomposition from oxygen. It is interesting to note the exceptional thermal stability of the complexed

(31) Hart, H.; Oku, A. *J. Org. Chem.* **1972**, *37*, 4269.

Scheme II

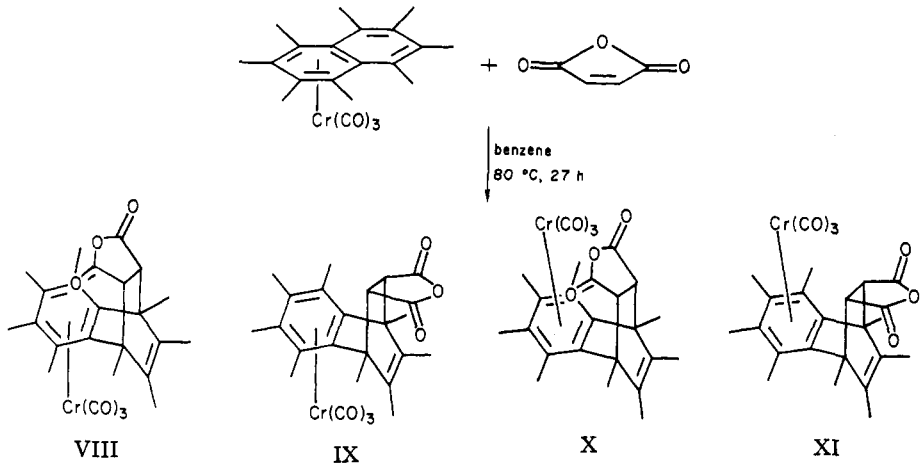

Table X. Summary of Diels-Alder Reaction of OMN with Maleic Anhydride

ref	[OMN]/[MA]	temp, °C	solvent	time, h	initial [OMN], M	combined % yield	exo/endo
31	1	132		13.5	1	50.3	2.0
30	1	110	none	24		91	7.0
30	0.5	155	none	6		60	4.4
30 (retro-Diels-Alder)	0.5	155	none	6	0	80	4.4
this work	0.20	80		66	0.150	81	7.14

Diels–Alder adducts relative to the free ligand.

Discussion

Ligand Substitution Reactions. The reactions involving a direct change in the ligand environment around the metal depend on the conditions. Thermally, substitution of the OMN occurs with $P(OCH_3)_3$ to give $Cr(CO)_3[P(OCH_3)_3]_3$. Photolysis, however, leads to the replacement of a carbon monoxide ligand. This difference between ground- and excited-state reactivities has been previously observed and was attributed to the idea that a one-electron excitation will have a greater impact on a two-electron donor compared to a six-electron donor.[32]

Diels–Alder Reaction. Distorted molecules such as octamethylnaphthalene usually exhibit greater reactivity relative to the unperturbed counterparts. One of the principle goals of this work was to evaluate the effect of metal complexation on this already unusual reactivity. The reaction which was chosen for evaluation was the cycloaddition of maleic anhydride. Since the original synthesis of OMN,[11] it was known to undergo Diels–Alder reactions. The details of this reaction and of the reactions of most of the polymethylnaphthalenes have since been studied.[30,31]

The conditions used in our experiments allowed a straight-forward sampling procedure for monitoring the reactions by high-pressure liquid chromatography and decreased the likelihood of any thermal decomposition of the metal complexes. In all the reactions conducted in benzene, arene exchange was never observed. In fact, the only time we did observe this reaction was during an attempted preparative liquid chromatographic purification of $(OMN)Cr(CO)_3$. When the material was eluted through a silica gel column (200–400 μm) with benzene, a mixture of $(\eta^6\text{-}C_6H_6)Cr(CO)_3$ and $(OMN)Cr(CO)_3$ was obtained. Despite the differences in our experimental conditions with those previously studied (Table X), the results agree reasonably well.

The corresponding reaction of maleic anhydride with $(OMN)Cr(CO)_3$ shows a greater than 2 orders-of-magnitude increase in the equilibrium constant. The nature of this 3–4-kcal/mol difference in energy for the complexed vs. the uncomplexed reaction is simply attributed to the weakened Cr–ring bond in the starting material. As the molecular structures clearly illustrate, all the Cr–C distances are longer in $(OMN)Cr(CO)_3$ relative to the product. In other words, as we proceed from starting material to product the enhanced strength of the Cr–C(arene) interaction must be added to the overall energy change of the reaction. This increased interaction of the Cr with the arene is allowed as the ring becomes planar. Extension of this idea to other reactions is straightforward. Any reaction in which the steric crowding of the peri methyls is relieved, complexation of a metal to the free ring should push the reaction in the forward direction. We are particularly interested in exploiting this effect to assist in the hydrogenation of OMN. As shown, the addition of H_2 to the free ring at the peri positions will relieve the crowding in this molecule (eq 3).

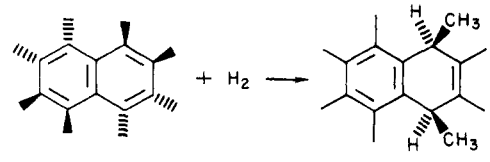

(3)

Acknowledgment is made to the Research Corp. and the University of Minnesota Graduate School for support of this research and to Du Pont Corp. for a Young Faculty Research Grant. We also gratefully acknowledge L. H. Pignolet and M. McGuiggan for assistance in the structural analyses and the NSF for partial support of our X-ray diffraction and structure-solving equipment (NSF Grant CHE 77-28505). We are grateful to H. Hart for commu-

(32) Geoffroy, G. L.; Wrighton, M. S. "Organometallic Photochemistry"; Academic Press: New York, 1979; p 79.

nicating his results prior to publication.

Registry No. (OMN)Cr(CO)$_3$, 79391-56-3; (OMN)Mo(CO)$_3$, 79391-57-4; (OMN)W(CO)$_3$, 79391-58-5; (OMN)Cr(CO)$_2$(PPh$_3$), 79391-59-6; (*endo*)-[OMN·MA]Cr(CO)$_3$, 79391-60-9; (*exo*)-[OMN·MA]Cr(CO)$_3$, 79434-50-7; (*endo*)-OMN·MA, 36744-72-6; (*exo*)-OMN·MA, 36744-73-7; Cr(CO)$_3$(P(OMe)$_3$)$_3$, 17764-72-6; Cr(CO)$_6$, 13007-92-6; (CH$_3$CN)$_3$Mo(CO)$_3$, 15038-48-9; (CH$_3$CN)$_3$W(CO)$_3$, 16800-47-8; MA, 108-31-6.

Supplementary Material Available: Listings of the observed and calculated structure factors used in the crystallographic analyses (21 pages). Ordering information is given on any current masthead page.

Further Studies on the Molecular Dynamics of the Four-Electron Bridging Carbonyl

John A. Marsella and Kenneth G. Caulton*

Department of Chemistry, Indiana University, Bloomington, Indiana 47405

Received July 14, 1981

Both Mn$_2$(CO)$_6$(dpm)$_2$, which contains only terminal carbonyls, and Mn$_2$(CO)$_5$(dpm)$_2$, which contains one μ:η^2 (four-electron donor) carbonyl, are shown to be fluxional by ^{13}C NMR spectroscopy. Scrambling in the hexacarbonyl occurs over both metal atoms with E_a = 10.2 kcal/mol and log A = 12.1, while that in pentacarbonyl involves only a wagging motion which results in disruption of the Dewar–Chatt portion of the four-electron donor carbonyl with E_a = 17.0 kcal/mol and log A = 15.0. By selective ^{31}P decoupling experiments, the chemical shift of the four-electron donor carbonyl is shown to fall in the chemical shift region normally attributed to terminal carbonyls. Coupling of ^{13}C to ^{31}P is small (<5 Hz) through the Dewar–Chatt portion of this type of carbonyl.

Introduction

The four-electron-donor carbonyl bridge, depicted formally as I, is an organometallic structural unit of relatively

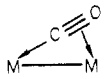

I

recent vintage. The first example, contained in Mn$_2$(CO)$_5$(dpm)$_2$, II (dpm = bis(diphenylphosphino)methane,

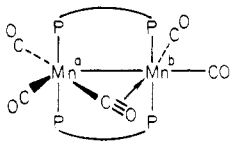

II

Ph$_2$PCH$_2$PPh$_2$), was reported in 1975 by Colton, Commons, and Hoskins.[1] The five carbonyls in this molecule are coplanar. Subsequent reports include Cp$_2$NbMo(CO)$_3$Cp,[2] Cp$_2$Zr(OC)(OCMe)Mo(CO)Cp,[3] and (C$_5$Me$_5$)$_2$ZrCo(CO)$_2$(C$_5$H$_5$).[4] A cluster-bound analogue occurs in HFe$_4$(CO)$_{13}^-$, where one of the carbonyl ligands donates a total of four electrons to all four iron atoms in Fe$_4$(CO)$_{13}$H$^-$.[5] Finally an extreme example of carbonyl Lewis basicity is found in Cp$_3$Nb$_3$(CO)$_7$, where one CO ligand lies obliquely over the Nb$_3$ triangle and donates via the carbon lone pair and *both* filled C≡O π orbitals.[6]

Carbon monoxide assumes the μ_2:η^2 functionality in ligand-deficient situations; indeed, this structural unit is generally formed by thermal or photochemical processes which expel ligands (e.g., CO or CH$_4$). Since such ligand-deficient situations are precisely those found on lightly loaded metal surfaces, molecular examples of multipoint attachment of CO represent an important opportunity to examine the dynamics and reactivity of a catalytically relevant moiety by use of spectroscopic methods.

Several years ago, we reported the results of a ^{31}P NMR study of Mn$_2$(CO)$_5$(dpm)$_2$ which indicated that the migrational processes depicted in eq 1 (bridging dpm ligands

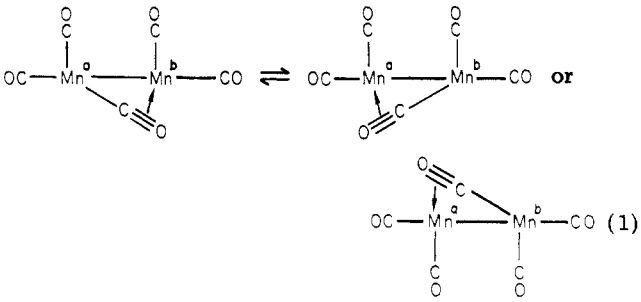

(1)

are omitted for simplicity) are *not* facile.[7] The observed inequivalence (at 30 °C) of the phosphorus nuclei attached to different manganese atoms allowed us to set a lower limit of 15.6 kcal/mol for the activation energy of eq 1. This result is compatible with the notion that multipoint carbonyl binding inhibits the characteristically facile migrations of two-electron donor carbonyls.

We were therefore somewhat surprised by our more recent result that *reorientation* of the six-electron donor carbonyl in Cp$_3$Nb$_3$(CO)$_7$ (eq 2) occurs with an activation energy, E_a, of 17 kcal/mol.[8] In order to examine this situation more critically, we have returned to perhaps the

(1) (a) Commons, C. J.; Hoskins, B. F. *Aust. J. Chem.* **1975**, *28*, 1663. (b) Colton, R.; Commons, C. J. *Ibid.* **1975**, *28*, 1673.
(2) Pasynskii, A. A.; Skripkin, Yu. V.; Eremenko, I. L.; Kalinnikov, V. T.; Aleksandrov, G. G.; Andrianov, V. G.; Struchkov, Yu. T. *J. Organomet. Chem.* **1979**, *165*, 49.
(3) Longato, B.; Norton, J. R.; Huffman, J. C.; Marsella, J. A.; Caulton, K. G. *J. Am. Chem. Soc.* **1981**, *103*, 209.
(4) Barger, P. T.; Bercaw, J. E. *J. Organomet. Chem.* **1980**, *201*, C39.
(5) Manassero, M.; Sanasoni, M.; Longoni, G. *J. Chem. Soc., Chem. Commun.* **1976**, 919.
(6) Herrmann, W. A.; Biersack, H.; Ziegler, M. L.; Weidenhammer, K.; Siegel, R.; Rehder, D. *J. Am. Chem. Soc.* **1981**, *103*, 1692.
(7) Caulton, K. G.; Adair, P. *J. Organomet. Chem.* **1976**, *114*, C11.
(8) Lewis, L. N.; Caulton, K. G. *Inorg. Chem.* **1980**, *19*, 3201.

0276-7333/82/2301-0274$01.25/0 © 1982 American Chemical Society